

## 11. PETROLOGY AND CHEMISTRY OF BASALTS FROM THE NAZCA PLATE: PART 1—PETROGRAPHY AND MINERAL CHEMISTRY

Colin H. Donaldson, Lunar Science Institute, Houston, Texas, and University of St. Andrews, Scotland  
Roy W. Brown, Lockheed Electronics Corporation, Houston, Texas  
and  
Arch M. Reid, NASA Johnson Space Center, Houston, Texas

### INTRODUCTION

We report on the petrography and mineral chemistry of 21 basalt samples drilled during Leg 34 of the Deep Sea Drilling Project from the Nazca plate. The suite of samples comprises 13 from Hole 319A, 3 from Hole 320B, and 5 from Site 321. The same samples have also been analyzed for major, minor, and trace element contents (Rhodes et al., this volume). Results of petrographic observations and electron microprobe analyses are summarized in Tables 1-6 and Figures 1-10.

### RESULTS

Table 1 lists the catalog numbers of the samples and their locations in cooling units and summarizes the rock types, textures, and range of compositions for the three principal phases—plagioclase, augite, and olivine. Rock types are distinguished on the basis of the groundmass grain size (medium grained [1-5 mm] versus fine grained [ $<1$  mm]) and phenocryst assemblage. Many of the rocks contain phenocrysts, the most abundant of which is plagioclase, followed by olivine. One sample, 319A-6-1, 84-89 cm, contains pyroxene microphenocrysts. In the groundmass, elongate (in some cases, skeletal) plagioclase laths are set in a cryptocrystalline matrix, or form an ophitic or intergranular texture with pyroxene, or form an intersertal texture. All three of these textures coexist in some samples (e.g., 319A-4-1, 129-132 cm). Groundmass olivine is present only in the finer grained rocks from Holes 319A and 320B and is totally absent in samples from Site 321. The groundmass olivines are subophitically enclosed by plagioclase laths (Figure 4). They are particularly susceptible to alteration to dark brown smectite. Each olivine grain may be either completely replaced or mantled by smectite (Figure 4). Those rocks in Table 1 for which the groundmass olivine column is labelled “none” contain neither groundmass crystals nor smectite crystals which could be inferred to be pseudomorphs after olivine. None of the samples contained glass. However, samples with intersertal texture contain abundant smectite, assumed to be the alteration product of glass and its associated devitrification products. Therefore, despite the low water contents and oxidation ratios of the Leg 34 basalts (Hart et al., 1974; Rhodes et al., this volume), relative to most other basalts recovered by the Deep Sea Drilling Project, the rocks are not mineralogically fresh.

Plagioclase phenocrysts have two types of occurrences—either isolated in the groundmass or, more commonly in glomerophytic units (Figure 5), some of which also contain olivine. The cores of these crystals ( $An_{87-68}$ )

are either unzoned or are oscillatory zoned with adjacent zones differing by 1-4 mol percent An. The margins of crystals in contact with the groundmass are continuously normal zoned. The periphery of each phenocryst has the same composition as the margins of groundmass plagioclase laths, which are always normally zoned from core ( $An_{75-63}$ ) to rim ( $An_{61-27}$ ). Fe content of both phenocryst and groundmass plagioclase is substantial (i.e., 0.3-1.0 wt%) and increases with Ab content of the plagioclase (Table 3). Plagioclase zoning is much more extensive in medium-grained rocks than in fine-grained rocks (Table 1).

Olivine phenocrysts have limited ranges of core composition ( $Fo_{89-84}$ , Tables 1 and 2). An unzoned core is typically surrounded by a narrow normally zoned mantle. Groundmass olivines are slightly zoned (Table 2) and generally are 1-3 mol % less forsterite-rich than the core of the phenocrysts in the same rock. The CaO contents of both phenocrystic and groundmass olivines exceed 1000 ppm (Table 2). The Ca content tends to increase with fayalite content of the olivine.

All the pyroxenes studied are augites. At Hole 319A and Site 321, pyroxenes have wide ranges of composition (Figure 10 and Table 4). Pyroxene in the rocks from Hole 320B is very fine grained and only three grains, all in one sample, were analyzed (Table 4). Augite compositions from individual rocks plotted in the pyroxene quadrilateral define either quench trends (cf Evans and Moore, 1968) or trends subparallel to, and slightly less calcic than, the Skaergaard trend. Some single ophitic crystals in the coarse-grained rocks are extensively zoned with respect to Fe-Mg content (Table 4). The microphenocrysts in Sample 319A-6-1, 84-89 cm are similar in major element composition to the earliest augite to crystallize in the Skaergaard intrusion (Figure 10).

The opaque phases are Fe-Ti oxides that occur in the groundmass, commonly as very small skeletal or dendritic crystallites. Titanomagnetite with around 25 wt%  $TiO_2$  is present in virtually all of the basalts and is accompanied by ilmenite in more than half of the samples (Table 5). Only one sample (320B-3-1, 120-125 cm) has a small euhedral Mg-Al-Cr spinel grain (Table 6) which is enclosed by early plagioclase. All other samples lack a Cr-spinel phase, a deficiency which is atypical of most mid-ocean-ridge basalts.

### CONCLUSIONS

Basalts at Site 321 lack both phenocryst and groundmass olivine (Table 1; contrast Holes 319A and 320B); also, the plagioclase phenocrysts are much less calcic

TABLE 1  
Summary of Samples Investigated, Rock Types Present and Their Textures, and the Range of Phase Composition in Each Rock

Sample (Interval in cm)	Cooling Unit <sup>a</sup>	Rock Type	Olivine Phenocryst <sup>b</sup> (Fo mol %)	Olivine Groundmass (Fo mol %)	Plagioclase Phenocryst (Core) <sup>c</sup>			Plagioclase Groundmass <sup>d</sup>			Augite <sup>e</sup>			Comments
			An	Ab (mol %)	Or	An	Ab (mol %)	Or	Ca	Mg (atomic props.)	Fe			
319A-1-1, 138-142	2	Fine-grained basalt	None	85				73.1-65.4	26.8-34.3	0.1-0.3	33-35.8	58-49.8	8.7-14.4	Skeletal olivine (0.1 mm across) and glomerophytic units of plagioclase (0.5 × 0.05 mm) subophitically enclosed by augite (0.1 mm across) set in cryptocrystalline matrix (fig. 1)
319A-2-2, 114-117	3	Medium-grained feldspar phryic basalt	None	None	81.9-73.4	17.9-26.3	0.2-0.3	63.8-34.8	35.9-64.6	0.3-0.6	34.6-43.6	40.4-43.4	25.0-13.0	Plagioclase phenocrysts and glomerocrysts set in groundmass of intergranular and intersertal texture
319A-3-2, 14-17	3	Medium-grained feldspar phryic basalt	None	None	74.8-69.6	24.9-29.9	0.3-0.5	64.4-32.6	35.3-66.7	0.3-0.7	35.4-41.9	52-46.7	12.6-11.3	Plagioclase phenocrysts (up to 1.5 mm across) and glomerocrysts set in groundmass of poikilophitic and intersertal textures (fig. 2)
319A-3-2, 127-130	3	Medium-grained feldspar phryic basalt	None	None	78.8-67.5	21.0-32.1	0.2-0.4	66.0-36.0	33.6-63.3	0.4-0.7	40-36	50-37	10-27	Texture similar to Sample 319A-3-2, 14-17 cm
319A-3-3, 46-49	3	Medium-grained feldspar phryic basalt	None	None	85.1-76.9	14.6-22.9	0.3-0.2	73.2-31.7	26.4-67.5	0.4-0.7	41.3-36.5	43.6-50.8	15.1-12.8	Texture similar to Sample 319A-3-2, 14-17 cm
319A-3-3, 106-109	3	Medium-grained feldspar phryic basalt	None	None	77.8-72.5	22.0-27.4	0.2	65.7-37.0	34.0-62.6	0.3-0.4	41-31.3	46-44.1	13-24.6	Texture similar to Sample 319A-3-2, 14-17 cm
319A-3-4, 18-21	4	Medium-grained olivine feldspar phryic basalt	85.4-71	80.0-76.0	85.0-80.1	14.7-19.8	0.3-0.1	66.3-27.3	33.5-72.0	0.2-0.7	39-32	44.7-43.5	16.1-24.5	Olivine phenocrysts (up to 3 mm across), plagioclase phenocrysts (up to 1.5 mm across), plagioclase glomerocrysts, and olivine-plagioclase glomerocrysts (troctolite, fig. 3) set in Groundmass textures identical to Sample 319A-3-2, 14-17 cm
319A-3-4, 100-103	4	Medium-grained feldspar phryic basalt	None	None	77.9	21.9	0.2	75.4-33.2	24.3-66.2	0.3-0.6	43.2-34.2	43.9-48.7	12.9-17.1	
319A-3-5, 37-41	5	Medium-grained olivine feldspar phryic basalt	88.8-79.5	None	80.5-75.1	9.3-24.7	0.2	65.4-30.6	34.2-68.8	0.3-0.6	41-37.3	47.2-45.2	11.7-17.6	Texture similar to Sample 319A-3-2, 14-17 cm
319A-4-1, 129-132	5	Fine-grained olivine feldspar basalt	88-79	81.3	80.5-77.9	9.4-22.0	0.1-0.2	65.8-34.2	33.8-65.1	0.4-0.8	44.2-29.4	44.2-43	11.1-27.5	Olivine phenocrysts (up to 3 mm across), plagioclase phenocrysts (up to 1.3 mm across), plagioclase glomerocrysts, and olivine-plagioclase glomerocrysts (troctolite fragments) set in groundmass of ophitic, intergranular and intersertal textures; Small grains of olivine scattered through matrix (fig. 4)
319A-5-1, 76-79	5	Fine-grained olivine feldspar	83.5-80.5	81.1	86.7-74.6	3.0-25.2	0.2-0.1	63.3-39.2	36.4-60.3	0.3-0.5	41.2-36.2	47.7-41.6	11.1-22.2	Texture similar to Sample 319A-4-1, 129-132 cm
319A-6-1, 84-89	7	Fine-grained pyroxene feldspar phryic basalt	None	None	82.1-70.6	17.7-29.1	0.2-0.3	63.3-60.0	36.3-39.6	0.4	41.5	49.7	8.7 (phenocrysts only analyzed; groundmass pyroxene too small for analysis)	Plagioclase phenocrysts (up to 3 × 1 mm) and glomerocrysts (fig. 5) and pyroxene glomerocrysts (up to 0.3 mm across, fig. 6) set in groundmass of felited plagioclase laths, cryptocrystalline material, and altered glass
319A-7-1, 119-122	8	Fine-grained olivine feldspar phryic basalt	84.0-81.5	83.0	78.8-73.2	21.0-26.6	0.2	69.1-39.6	30.7-59.9	0.2-0.5	42	48-43	10-15	Texture similar to Sample 319A-5-1, 76-79 cm

320B-3-1, 120-125	Fine-grained olivine feldspar microphyric basalt	None	85.0-81.0	76.3	23.4	0.3	71.2-61.3	28.5-38.0	0.4-0.7	No pyroxene	Plagioclase microphenocrysts (up to 1 mm across), skeletal olivines (0.5 mm) and glomerophyric units of plagioclase laths ( $1 \times 0.1$ mm) subophitically enclosed by olivine (0.5 mm across) set in cryptocrystalline groundmass	
320B-4-1, 130-133	Fine-grained feldspar microphyric basalt	None	None	69.7-67.2	29.9-32.5	0.4	68.4-46.9	31.2-52.4	0.4-0.8	37.5-30	46.5-54	16
320B-5-1, 117-123	Fine-grained feldspar phryic basalt	None	None	69.4	30.1	0.2	70.7-49.1	29.1-50.0	0.3-0.9	No pyroxene	Skeletal plagioclase microphenocrysts (up to $1 \times 0.3$ mm) set in groundmass of felted plagioclase laths ( $0.2 \times 0.05$ mm) and cryptocrystalline material (fig. 7)	
321-13-4, 119-124	Fine-grained feldspar microphyric basalt	None	None	69.8-67.0	30.0-32.3	0.2-0.6	64.2-56.2	35.4-42.3	0.4-1.5	39.8-34	45-48	15.5-18
321-14-1, 99-102	Aphyric basalt	None					64.8-45.2	34.7-54.1	0.4-0.7	37.6-32.5	42.2-51.6	20.2-15.8
321-14-2, 127-130	Fine-grained feldspar phryic basalt	None N	None	70.4	29.2	0.3	68.0-38.1	31.6-60.8	0.4-1.1	35.4-30	45.7-43.5	18.8-26.5
321-14-3, 93-96	Fine-grained feldspar phryic basalt	None	None	68.7	31.0	0.3	67.9-46.1	31.7-53.2	0.4-0.7	30-32	50-47	20-21
321-14-4, 61-64	Aphyric basalt	None					65.2-47.8	34.3-51.1	0.6-1.1	37-28	49.5-52	13.5-20

<sup>a</sup>Identified by shipboard scientists. Numbering system that of Rhodes et al. (this volume).<sup>b</sup>Core and rim compositions.<sup>c</sup>Range of core compositions.<sup>d</sup>Most calcic core and most sodic rim compositions.<sup>e</sup>Most magnesian and least magnesian augite.

TABLE 2  
Olivine Compositions in Selected Leg 34 Samples

319A-1-1, 138-142 cm				319A-3-4, 18-21 cm							
	Skeletal Grains	Phenocryst Core	Phenocryst Rim		Groundmass Core	Groundmass Rim		Phenocryst Core	Phenocryst Rim	Groundmass Core	Groundmass Rim
SiO <sub>2</sub>	39.90	39.61	39.27	38.58	39.37	38.80	39.76	37.26	38.88	38.06	
FeO	13.93	13.93	16.40	21.28	18.44	18.36	13.66	25.80	18.31	22.07	
MnO	0.23	0.25	0.23	0.35	0.32	0.43	0.19	0.36	0.28	0.38	
MgO	45.10	45.11	43.37	39.48	41.71	41.90	45.45	35.90	41.81	38.81	
NiO	0.14	0.14	0.19	0.15	0.17	0.14	0.19	0.11	0.14	0.14	
CaO	0.31	0.28	0.26	0.33	0.28	0.26	0.26	0.31	0.32	0.35	
Total	99.61	99.32	99.72	100.17	100.29	99.89	99.51	99.74	99.74	99.81	
Fo mol %	85	85	82	77	80	80	85.5	71	80	76	
319A-3-5, 37-41 cm						319A-4-1, 129-132 cm					
Grains in Troctolite Fragment			Phenocryst Rim	Phenocryst Core	Phenocryst	Phenocryst Core	Phenocryst Rim	Phenocryst	Phenocryst	Groundmass	Groundmass
SiO <sub>2</sub>	39.21	39.34	39.93	40.74	40.49	39.85	39.66	38.52	39.63	40.28	38.92
FeO	15.76	16.05	13.63	13.36	10.57	12.96	12.88	19.06	12.79	11.34	17.22
MnO	0.22	0.20	0.21	0.30	0.21	0.17	0.18	0.39	0.20	0.18	0.26
MgO	43.74	43.59	45.12	45.50	47.63	45.79	45.76	40.46	45.54	46.66	42.30
NiO	0.21	0.17	0.16	0.19	0.14	0.16	0.19	0.14	0.15	0.20	0.14
CaO	0.31	0.29	0.30	0.33	0.24	0.23	0.26	0.34	0.28	0.24	0.29
Total	99.45	99.64	99.35	100.42	99.28	99.16	98.93	98.91	98.59	98.90	99.13
Fo mol %	83	83	85.5	86	89	86	86	79	86	88	81
319A-5-1, 76-79 cm				319A-7-1, 119-122 cm				320B-3-1, 120-125 cm			
Phenocryst		Groundmass	Groundmass	Phenocryst	Groundmass	Groundmass	Core	Groundmass	Groundmass	Groundmass	Groundmass
SiO <sub>2</sub>	39.23	39.14	39.18	38.80	39.25	39.20	39.06	39.06	39.30	39.56	39.65
FeO	15.35	16.84	17.75	17.24	15.40	14.96	15.94	16.84	14.30	14.64	14.33
MnO	0.26	0.30	0.27	0.28	0.25	0.20	0.25	0.27	0.22	0.26	0.21
MgO	44.22	42.78	41.94	42.16	43.92	44.23	43.27	42.37	44.60	44.56	44.67
NiO	0.14	0.15	0.17	0.14	0.15	0.18	0.12	0.12	0.21	0.22	0.16
CaO	0.26	0.30	0.23	0.33	0.31	0.34	0.32	0.37	0.35	0.27	0.30
Total	99.46	99.51	99.54	98.95	99.28	99.11	98.96	99.03	98.98	99.51	99.32
Fo mol %	83.5	82	81	81	83.5	84	83	82	85	84	85

**TABLE 3**  
**Plagioclase Compositions in Selected Leg 34 Samples**

	319A-1-1, 138-142 cm				319A-2-2, 114-117 cm				319A-3-3, 46-49 cm				319A-3-5, 37-41 cm			
	Core	Rim	Core	Rim	Groundmass Core	Phenocryst Rim	Core	Rim	Groundmass Core	Rim	Core	Rim	Groundmass Core	Phenocryst Rim	Groundmass Core	
SiO <sub>2</sub>	50.73	50.91	51.78	51.20	52.52	56.45	48.68	60.55	47.47	60.41	52.57	59.69	52.13	50.49	59.39	48.20
Al <sub>2</sub> O <sub>3</sub>	31.52	31.18	30.94	31.75	30.31	27.61	32.74	23.41	33.68	24.22	29.95	24.16	30.33	31.82	26.17	33.50
FeO <sup>a</sup>	0.63	0.71	0.60	0.63	0.63	1.04	0.48	0.66	0.42	1.24	0.69	0.60	0.64	0.54	0.74	0.39
CaO	14.39	14.31	13.96	13.03	12.69	8.53	16.14	6.15	16.70	6.16	14.45	6.17	12.91	14.71	6.17	15.94
Na <sub>2</sub> O	3.01	3.07	3.17	3.88	4.05	6.22	2.03	7.73	1.65	7.33	2.99	7.53	3.85	2.76	7.72	2.20
K <sub>2</sub> O	0.02	0.02	0.03	0.04	0.05	0.12	0.03	0.11	0.04	0.12	0.06	0.10	0.05	0.03	0.10	0.03
Total	100.30	100.20	100.48	100.53	100.25	99.97	100.10	98.61	99.96	99.48	100.71	98.25	99.91	100.35	100.29	100.26
An mol %	73	72.5	71	65	64	43	82	30.5	85	32	73	31	65	75	80	81

	319A-4-1, 129-132 cm				319A-6-1, 84-89 cm				319A-7-1, 119-122 cm				320B-5-1, 117-123 cm						
	Groundmass Core	Rim	Groundmass Core	Phenocryst Rim	Phenocryst Core	Rim	Groundmass Core	Phenocryst Core	Rim	Groundmass Core	Phenocryst Rim	Phenocryst Core	Rim	Groundmass Core	Rim	Phenocryst Core	Rim		
SiO <sub>2</sub>	53.92	58.36	52.50	48.85	57.68	48.59	51.70	53.26	53.86	50.58	57.19	49.21	55.16	51.79	54.91	52.08	53.88	52.33	54.93
Al <sub>2</sub> O <sub>3</sub>	29.23	26.59	30.39	33.10	26.66	33.22	31.05	29.86	28.86	30.80	26.89	32.75	28.37	30.91	28.74	31.02	29.56	30.66	28.98
FeO <sup>a</sup>	0.83	1.04	0.69	0.41	0.92	0.40	0.66	0.96	1.12	0.96	1.14	0.42	1.24	0.54	0.97	0.58	0.91	0.62	0.99
CaO	11.19	6.91	12.40	15.35	8.11	16.12	11.81	12.10	12.02	14.27	9.52	15.46	9.12	13.90	9.29	10.51	10.51	13.29	11.08
Na <sub>2</sub> O	4.57	7.35	3.63	2.13	6.31	2.00	4.42	4.24	4.28	2.97	5.81	2.37	6.00	3.41	5.85	5.10	5.13	3.66	5.07
K <sub>2</sub> O	0.04	0.13	0.06	0.01	0.07	0.03	0.07	0.07	0.11	0.03	0.05	0.02	0.07	0.06	0.12	0.11	0.06	0.06	0.06
Total	99.78	100.38	99.67	99.85	99.75	100.36	99.71	100.49	100.25	99.61	100.60	100.23	99.96	100.61	99.88	99.40	100.10	100.62	101.11
An mol %	58	34	66	80.5	42	82	60	61.5	61	73	48	79	46	70	47	53	53	67	55

	320B-4-1, 130-133 cm				321-14-1, 99-102 cm				321-14-2, 127-130 cm								
	Groundmass Core	Phenocryst Core	Rim	Groundmass Core	Rim	Groundmass Core	Rim	Groundmass Core	Rim	Phenocryst Core	Rim	Phenocryst Core	Rim	Groundmass Core	Rim	Phenocryst Core	Rim
SiO <sub>2</sub>	51.44	51.76	53.46	54.01	59.26	54.06	56.16	53.29	56.76	51.10	58.81						
Al <sub>2</sub> O <sub>3</sub>	31.52	30.99	29.61	29.37	25.98	29.42	28.06	29.31	27.59	30.96	26.32						
FeO <sup>a</sup>	0.59	0.57	0.87	0.92	0.88	0.94	1.11	0.85	0.94	0.71	0.84						
CaO	13.94	13.56	9.79	12.55	8.91	11.69	9.86	12.65	9.31	13.95	7.54						
Na <sub>2</sub> O	3.28	3.45	5.61	3.84	5.99	4.37	5.42	4.13	5.40	3.38	6.74						
K <sub>2</sub> O	0.04	0.04	0.14	0.07	0.11	0.06	0.09	0.06	0.12	0.06	0.18						
Total	100.81	100.37	99.48	100.76	101.13	100.54	100.70	100.23	100.62	100.16	100.43						
An mol %	71	69	49	65	45	60	50.5	63	47	70	38						

<sup>a</sup>All iron as FeO.

TABLE 4  
Pyroxene Compositions in Selected Leg 34 Samples

319A-2-2, 114-117 cm						319A-3-2, 14-17 cm						319A-3-4, 100-103 cm						319A-3-5, 37-41 cm						319A-6-1, 84-89 cm					
						Core	Rim					Core	Rim			Core	Rim			Core	Rim			Core	Rim				
SiO <sub>2</sub>	49.77	49.94	48.72	51.21	51.05	50.93	50.71	49.66	50.99	51.50	51.96	50.50			50.41	52.03	53.02	51.39											
TiO <sub>2</sub>	1.42	1.39	1.86	1.01	1.05	0.96	1.02	1.24	1.04	0.73	0.89	1.23			1.51	0.67	0.50	0.96											
Al <sub>2</sub> O <sub>3</sub>	3.48	3.08	4.86	3.48	3.74	3.49	3.44	2.52	3.03	1.29	2.42	3.88	3.83	3.83	2.93	2.46	4.17												
Cr <sub>2</sub> O <sub>3</sub>	0.24	0.07	0.22	0.30	0.32	0.35	0.39	0.02	0.19	0.10	0.06	0.18			0.13	0.59	0.57	0.43											
FeO <sup>a</sup>	9.61	11.05	9.00	6.86	6.69	6.81	8.48	8.88	8.79	10.70	8.54	8.37	(10.63)	8.93	6.72	6.91	7.08												
MnO	0.23	0.28	0.20	0.17	0.16	0.16	0.23	0.34	0.25	0.24	0.21	0.24			0.21	0.18	0.15	0.16											
MgO	14.97	15.16	20.58	16.32	16.71	16.47	15.69	15.47	15.80	17.02	15.82	16.29	(15.50)	15.70	17.44	17.85	19.06												
CaO	18.82	18.11	13.98	19.82	19.65	19.71	19.26	18.97	18.32	16.50	19.09	18.54	(17.77)	18.73	19.37	19.50	17.95												
Na <sub>2</sub> O	0.33	0.30	0.35	0.27	0.27	0.27	0.32	0.32	0.31	0.23	0.28	0.17			0.28	0.25	0.25	0.26											
Total	99.87	99.38	99.77	99.44	99.64	99.15	99.54	97.42	98.72	98.31	99.27	99.40			99.73	100.19	101.20	101.48											
Wo	39.9	37.9	28.2	41.4	40.8	41.1	40.4	40.0	38.8	34.0	40.0	38.8	(37.3)	39.4	39.6	39.2	35.9												
En	44.2	44.1	57.7	47.4	48.3	47.8	45.8	45.4	46.6	48.8	46.1	47.5	(45.3)	45.9	49.6	49.9	53.0												
Fs	15.9	18.0	14.2	11.2	10.9	11.1	13.9	14.6	14.5	17.2	14.0	13.7	(17.4)	14.7	10.7	10.8	11.1												
319A-7-1, 119-122 cm						320B-5-1, 117-123 cm						321-13-4, 119-124 cm						321-14-4, 61-64 cm											
SiO <sub>2</sub>	49.30	52.83	49.67	49.65	50.54	50.88	52.22	50.54	51.14	52.25	50.57	51.45	48.58	50.22															
TiO <sub>2</sub>	1.66	0.67	1.50	1.46	1.31	0.98	0.96	1.11	0.94	0.53	1.08	0.86	1.67	1.18															
Al <sub>2</sub> O <sub>3</sub>	4.66	1.63	5.07	4.40	4.18	3.74	3.49	4.29	2.95	1.44	3.39	2.29	3.30	3.20															
Cr <sub>2</sub> O <sub>3</sub>	0.13	0.05	0.36	0.12	0.26	0.29	0.14	0.18	0.20	0.12	0.26	0.04	0.01	0.07															
FeO <sup>a</sup>	9.11	10.97	7.55	9.10	9.30	8.53	10.14	9.18	8.59	9.34	8.86	8.43	13.13	10.01															
MnO	0.20	0.29	0.18	0.26	0.22	0.24	0.27	0.29	0.25	0.27	0.20	0.32	0.27	0.23															
MgO	14.62	17.96	15.58	16.44	19.10	17.56	20.83	16.08	17.35	15.65	16.21	16.76	16.39	17.26															
CaO	19.74	16.36	19.94	16.95	14.48	16.57	12.16	17.29	17.32	18.85	18.05	17.55	14.30	16.22															
Na <sub>2</sub> O	0.32	0.23	0.31	0.28	0.23	0.22	0.21	0.16	0.20	0.16	0.22	0.20	0.24	0.22															
Total	99.74	101.00	100.15	98.66	99.62	99.01	100.42	99.12	98.94	98.61	98.84	97.70	97.89	98.61															
Wo	41.8	32.8	42.0	36.1	30.0	34.8	24.8	36.9	36.0	39.3	38.0	37.0	30.2	33.8															
En	43.1	50.1	45.6	48.7	55.0	51.3	59.1	47.8	50.1	45.4	47.5	49.1	48.2	50.0															
Fs	15.1	17.2	12.4	15.1	15.0	14.0	16.1	15.3	13.9	15.2	14.6	13.9	21.6	16.3															

<sup>a</sup>All iron as FeO.

TABLE 5  
Ilmenite and Titanomagnetite Compositions in Selected Leg 34 Samples

319A-3-2, 127-130 cm										319A-3-3, 106-109 cm					
TiO <sub>2</sub>	29.42	25.12	26.00	25.94	50.34	50.55	48.92	16.79	50.46	25.69	24.72				
Al <sub>2</sub> O <sub>3</sub>	1.89	2.00	1.55	1.41	0.11	0.00	0.06	1.69	0.10	2.08	2.03				
Cr <sub>2</sub> O <sub>3</sub>	0.04	0.04	0.02	0.03	0.02	0.00	0.02	0.04	0.00	0.03	0.03				
FeO <sup>a</sup>	65.36	67.95	69.29	67.29	49.37	47.24	49.31	74.35	49.28	66.70	67.89				
MnO	0.60	0.62	0.78	0.80	0.98	2.84	0.74	0.58	0.61	0.65	0.76				
MgO	0.36	0.65	0.30	0.27	0.62	0.26	0.53	0.24	0.84	1.01	0.48				
Total	97.67	96.38	96.94	95.74	101.44	100.89	99.58	95.69	101.29	96.16	95.91				
319A-2-2, 114-117 cm								319A-3-2, 14-17 cm							
TiO <sub>2</sub>	49.51	23.83	23.85	21.78	24.52	24.06	23.66	25.15	23.28	24.19	23.21	46.97	21.23	23.33	
FeO <sup>a</sup>	48.58	72.27	72.90	73.18	71.46	72.67	71.82	70.77	67.72	71.78	73.75	52.56	75.46	74.11	
MgO	0.05	0.51	0.33	0.22	0.49	0.44	0.52	0.83	0.86	0.49	0.33	0.33	0.17	0.29	
Total	98.94	96.61	97.08	95.18	96.47	97.17	96.00	96.75	91.86	96.46	97.29	99.86	96.86	97.73	
319A-3-4, 100-103 cm								319A-3-5, 37-41 cm							
TiO <sub>2</sub>	49.96	24.25	22.84	26.46	49.62	23.26	23.70	22.63	22.21	22.67	22.74	23.47	24.36	23.64	23.47
FeO <sup>a</sup>	47.61	71.39	73.27	69.17	49.41	72.65	72.32	73.63	74.04	73.76	73.94	72.15	72.77	71.10	71.64
MgO	1.55	0.95	0.69	0.96	0.44	0.64	0.38	0.67	0.50	0.47	0.31	0.45	0.55	0.46	0.62
Total	99.13	96.59	96.80	96.59	99.47	96.55	96.40	96.93	96.75	96.90	96.99	96.07	97.68	95.20	95.73
												321-14-1, 99-102 cm		321-14-2, 127-130 cm	

<sup>a</sup>All iron as FeO.

TABLE 6  
Spinel Composition in Sample  
320B-3-1, 120-125 cm

TiO <sub>2</sub>	1.08
Al <sub>2</sub> O <sub>3</sub>	24.45
Cr <sub>2</sub> O <sub>3</sub>	36.79
FeO <sup>a</sup>	23.73
MnO	0.22
MgO	13.32
Total	99.59

<sup>a</sup>All iron as FeO.

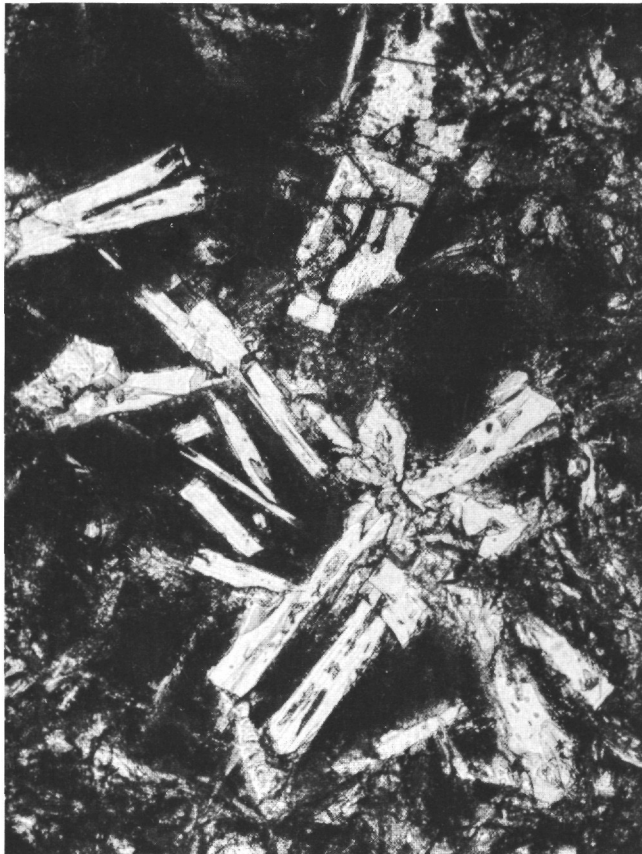


Figure 1. Skeletal olivine (top of photograph) and glomerocrysts of plagioclase laths and anhedral augite set in cryptocrystalline groundmass. 2 X 2.3 mm. Sample 319A-1-1, 138-142 cm.

than those in basalts at Hole 319A. Core compositions of groundmass plagioclases in Site 321 basalts are more sodic than those in samples from Hole 319A, and they have larger orthoclase contents (Table 1). These petrographic differences are not attributable to differences in cooling history between the basalts at the two sites. Rather, site 321 basalts are inferred to be more alkali rich than those in Hole 319A and to have had different crystallization histories. Although the core compositions of plagioclase phenocrysts in samples from Hole 320B are not as calcic as those of the most anorthite-rich plagioclases at Hole 319A, the rocks from both holes are similar in phase compositions (Table 1). The generally smaller range of phase zoning in rocks from Hole 320B reflects faster cooling.



Figure 2. Poikilophitic and intersertal texture typical of those in medium-grained basalts at Hole 319A. 1 X 1.3 cm. Sample 319A-3-3, 46-49 cm.

At each site, basalts from different cooling units and within individual cooling units have similar parageneses, except for crystallization of olivine. The absence of olivine phenocrysts from some of our samples from the thick cooling unit 3 (Table 1) may be due to crystal settling. Our companion paper (Rhodes et al., this volume) indicates that basalts at Site 319 are tholeiitic in composition rather than transitional to alkaline in affinity, as inferred in the preliminary report by the shipboard scientists from the occurrence of groundmass olivine. In the thick cooling unit (3, Table 1) groundmass olivine is absent from rocks at the center of the unit. As noted by Evans and Moore (1968), persistence of groundmass olivine in a tholeiite is favored by rapid cooling and hence is an unsatisfactory index of magma type.

Our petrographic observations suggest that basalts at Sites 319 and 320 are plagioclase-(olivine) tholeiites, while those at Site 321 are more fractionated tholeiites. We conclude that basalts from all three sites are oceanic tholeiites and products of ocean ridge volcanism.

#### ACKNOWLEDGMENTS

C.H. Donaldson thanks the Natural Environment Research Council of the United Kingdom for financial support and the Lunar Science Institute for a Visiting Graduate Fellowship. Mike Rhodes kindly reviewed the manuscript. The Lunar Science Institute is operated by the Universities Space Research

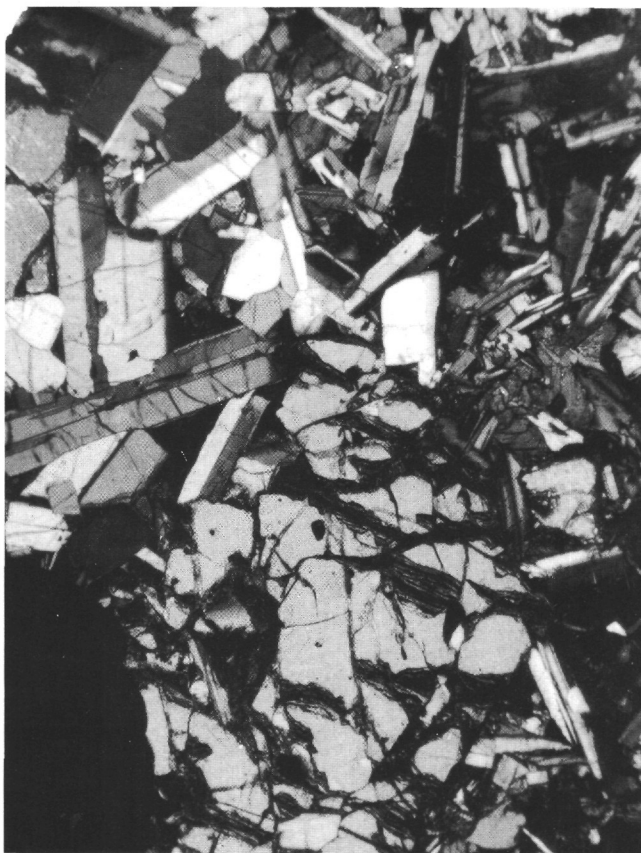


Figure 3. Troctolite xenolith in olivine-feldspar phryic basalt. Large olivine crystal poikilitically encloses plagioclase crystals (bottom of photograph). Groundmass (at right of photograph) consists of plagioclase and augite.  $5.2 \times 5.5$  mm. Polarized light. Sample 319A-3-5, 37-41 cm.

Association under Contract No. NSR-09-051-001 with NASA. This paper is Lunar Science Institute Contribution No. 198.

#### REFERENCES

Evans, B.W. and Moore, J.G., 1968. Mineralogy as a function of depth in the Prehistoric Makaopuhi tholeiitic lava lake, Hawaii: Contrib. Mineral. Petrol., v. 17, p. 97.



Figure 4. Groundmass olivine crystals (top center and lower center) trapped between plagioclase laths (white) which are subophitically enclosed by augite (gray). Note the dark rim of smectite around the olivine.  $2.1 \times 2.3$  mm. Sample 319A-4-1, 129-132 cm.

Hart, S.R., et al., 1974. Oceanic basalts and the Nazca plate: Geotimes, v. 19, p. 20-24.

Muir, I.D., 1951. The clinopyroxenes of the Skaergaard intrusion, eastern Greenland: Min. Mag., v. 29, p. 690.

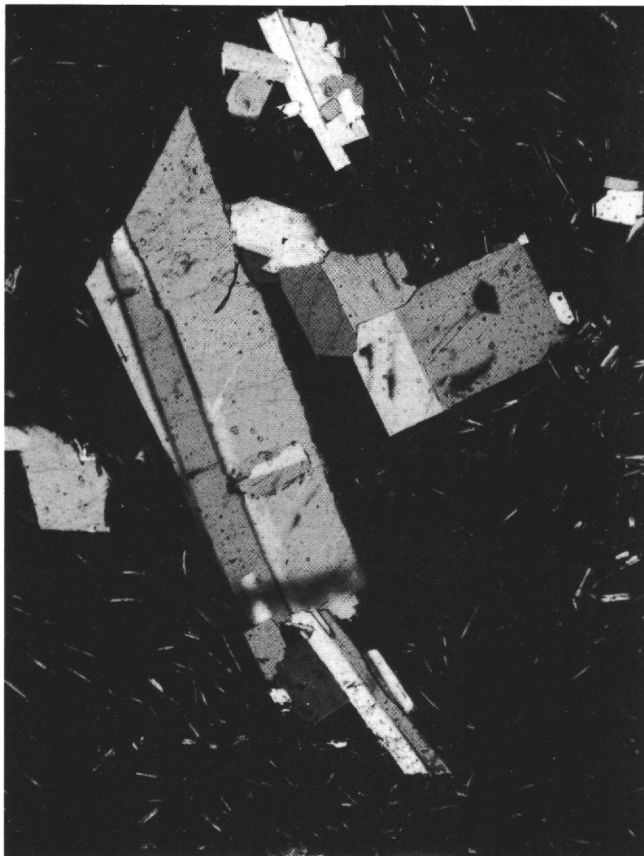


Figure 5. Glomerocrysts of plagioclase set in cryptocrystalline groundmass. 4 X 4.3 mm. Polarized light. Sample 319A-6-1, 84-89 cm.



Figure 6. Pyroxene microphenocryst and plagioclase lath set in a matrix of skeletal plagioclase laths and cryptocrystalline material. 1.5 X 1.7 mm. Sample 319A-6-1 84-89 cm.

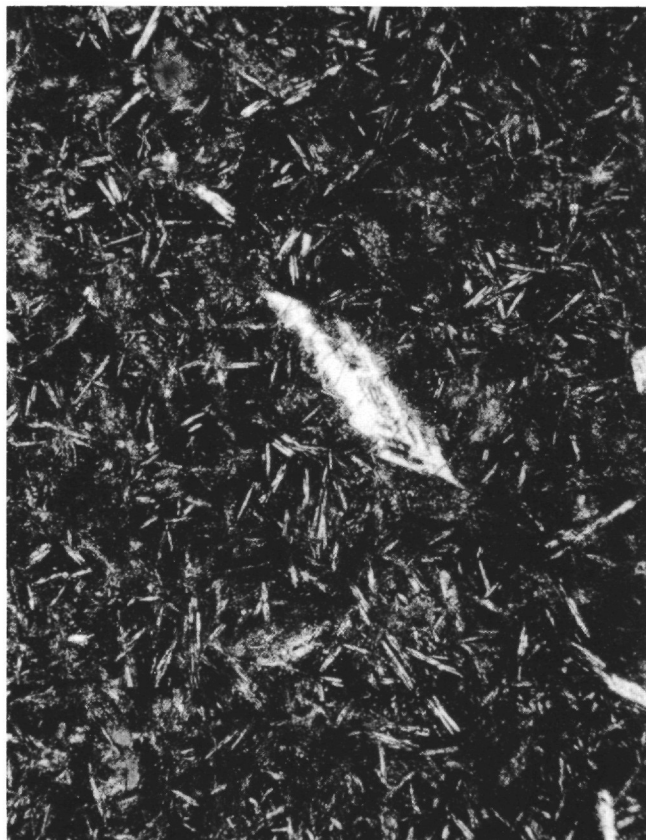


Figure 7. Skeletal plagioclase microphenocryst set in groundmass of felted plagioclase and cryptocrystalline material. 2 X 2.2 mm across. Sample 320B-4-1, 130-133 cm.



Figure 8. Intergranular texture of pyroxene and plagioclase in aphyric basalt. 1 X 1.2 mm. Polarized light. Sample 321-14-4, 61-64 cm.

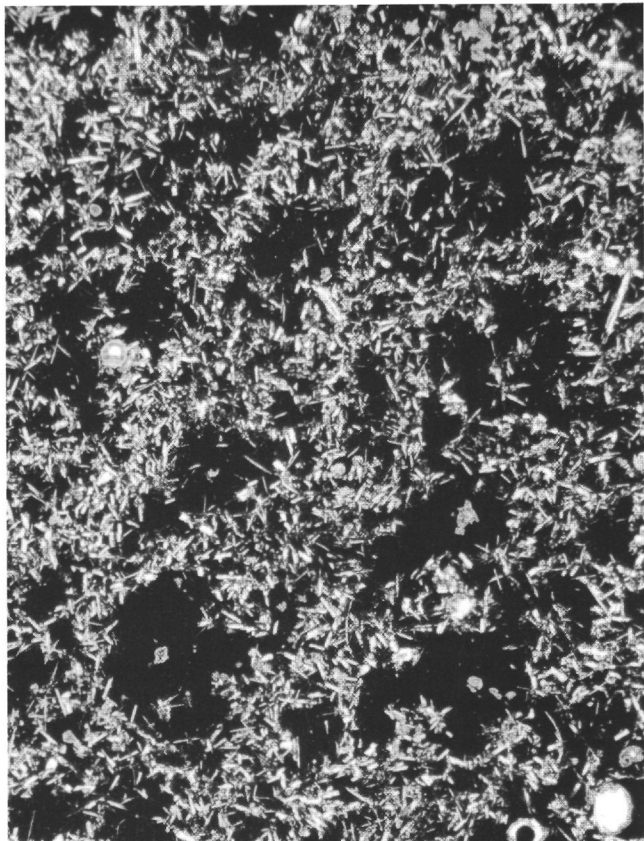


Figure 9. Intergranular and intersertal textures in groundmass of fine-grained feldspar phryic basalt.  $5.2 \times 5.5$  mm. Sample 321-13-4, 119-124 cm.

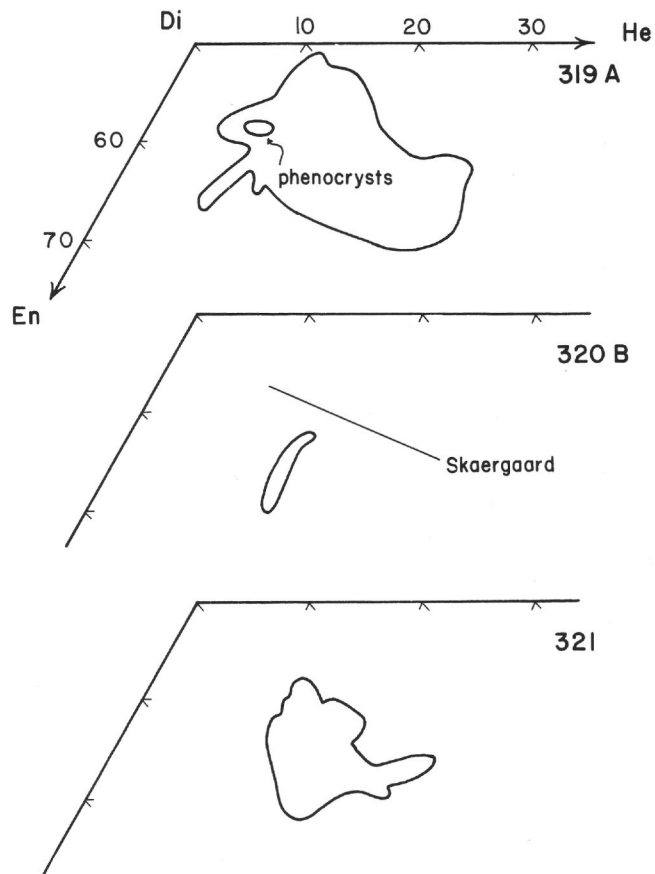


Figure 10. Summary of pyroxene compositions in samples from Holes 319A, 320B, and 321 plotted in the Di-He-En-Fs quadrilateral. Line on diagram for Hole 320B shows the trend of early crystallizing augite in the Skaergaard intrusion (Muir, 1941).